INTERNATIONAL JOURNAL OF MARITIME TECHNOLOGY
IJMT Vol.4/Summer2015 (1-9)
Available online at: http://ijmt.ir/browse.php?a_code=A-10-450-2&sid=1&slc_lang=en

Added Resistance of an AUV Moving Inside a Water Pipeline Due to Wall Proximity

*Mohammad Moonesun[1,2], Yuri Korol[2], Hosein Dalayeli[3],Asghar Mahdian[3], Anna Brazhko[2]

[1]MUT, Department of Marine Engineering, Shahinshahr, Iran;m.moonesun@gmail.com
[2]National University of Shipbuilding Admiral Makarov (NUOS), Department of Hydrodynamics,Ukraine
[3] MUT, Department of Mechanical Engineering, Shahinshahr, Iran

ARTICLE INFO

Article History:
Received: 2 Nov. 2015
Accepted: 17 Jan. 2016

Keywords:
AUV
Torpedo
Pipeline
Hydrodynamic
added resistance
wall effect

ABSTRACT

The present paper evaluates the added resistance of a torpedo shaped AUV - awing to the wall effect inside a pipe- moving inside a water pipeline. All around the world, there are long extending water or petroleum pipelines which require regular inspection by AUVs. In pipes, the AUV moves like as a torpedo in launcher. The pipes have limited diameter and because of the wall effects on the fluid flow around the AUV, the resistance will be significantly more than the free flow condition. For example the resistance of an AUV for d/D equal to 2, is about two times of the free stream. This added resistance should be accounted accurately because it is a necessary requirement for determination of vehicle speed, power demand, range and duration of operation. This paper considers a torpedo shape AUV moving inside the pipes with the different diameters. The resistance of this modeling will be compared to the resistance of free steam modeling. This study found that the ratio of d/D equal to 12 could be regarded as critical pipe diameter which added resistance is zero. In restricted diameter pipe the pressure resistance has a main role in total resistance about 45~90 percentages depending on the d/D ratio. This analysis is performed by Flow Vision (V.2.3) software based on CFD method and solving the RANS equations.

1. Introduction

Water or petroleum pipelines are extended all over the words with millions of kilometers long. A severe breakdown of a pipeline can lead to large costs and also lead to pollution and accidents. Hence routine inspection and maintenance of the pipelines are necessary for their trouble-free performance. Water supply is a basic public service and therefore, inspection tasks cannot compromise on the continuity or quality. Painumgal *et al*. [1] presented an inspection system which is capable of operating when the pipeline is in-service. Today several different pipeline inspection robots exist which are presented by Moghaddam [2], Harry [3], Bahmanyar [4], Muramatsu [5], Roh *et al*. [6,7] and Dadkhah [8]. The pipeline inspection robots presently are used by the contact with the walls for motion and positioning in the centre of the pipe (Okamoto[9]). Figure 1 (Painumgal *et al*. [1]) shows the Autonomous Underwater Vehicle (AUV) inside a pipeline. This is a simple AUV with conical ends, but today modern AUVs have usually torpedo shape. Discussion about submarine shape design is presented by Joubert [10,11], Moonesun [12,13], and Burcher [14]. The aim for developing this inspection system is to enable non-destructive and non-disruptive inspection of water pipelines. Recently torpedo shaped ocean going AUVs(Najjaran [17] and Jorg [18]) have been modified to inspect large pipelines. These vehicles have been used to inspect very huge pipeline shaving a diameter of more than 2 meters. It is important for the pipeline internal inspection robots to be able to enter and leave the pipeline with the least disruption or damage to the existing pipe systems. The larger the pipeline network, the greater the amount of inspection to be carried out. Hence autonomous and free operation is ideal for long distance inspection. Therefore, Autonomous Underwater Vehicles (AUV) are ideal tools for pipeline internal inspection (Painumgal *et al*. [1]).The flow field around a submarine inside a pipe or ducted space is different from the free stream. The proximity to the interior boundary of the hull induces wall effect on the fluid flow. In such cases, the boundary layer develops all over the circumference. The initial development of the boundary layer is similar to that occurring over the flat plate. At some distance from the entrance, the boundary layers merge and further changes in velocity

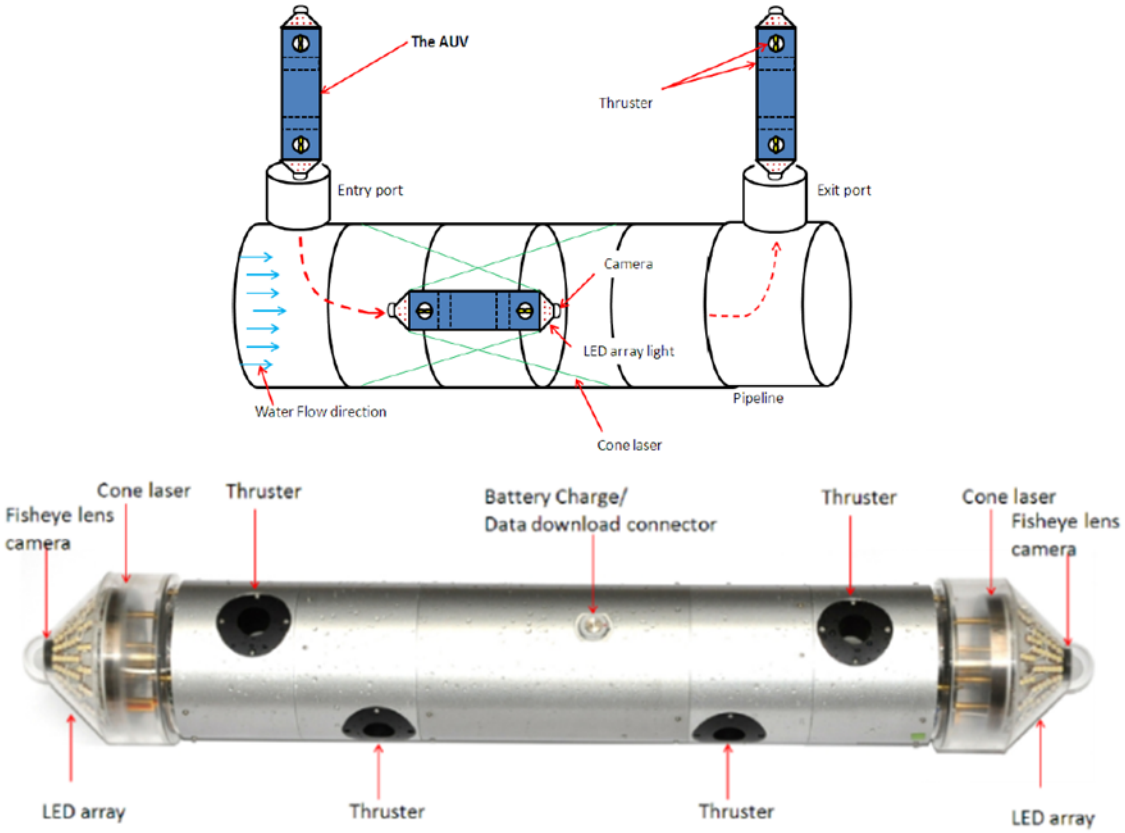

Figure 1. Schematic of pipeline inspection System and sample AUV (PICTAN) (Painumgal *et al.* [1])

distribution become impossible. The velocity profile beyond this point remains unchanged. The distance up to this point is known as the entry length which is about 0.04Re×d. The flow beyond this said to be fully developed. The velocity profiles in the entry region and the fully developed region are shown in Fig.2. The flow was observed to be laminar until a Reynolds number value of about 2300. The Reynolds number is calculated on the basis of the diameter (ud/ν). In the pipe flow, it is nota function of the length. As long as the diameter is constant, the Reynolds number depends upon the velocity for a given flow. Hence the value of velocity determines the nature of the flow in pipes for a given fluid. The value for the flow Reynolds number is decided by the diameter and the velocity. As shown in Fig.2, Region (A) is the non-viscous flow that is not affected by the boundary layer but Region (B) is the boundary layer region. The length, x, according to (Pritamashutosh[17]), can be calculated using the relation $x/D = 4.4R_e^{\frac{1}{6}}$. After this length, the flow within the boundary layer turns turbulent. A very thin laminar sub-layer near the wall in which the velocity gradient is linear is present all through. After some length the boundary layers merge and the flow becomes fully developed. The entry length in turbulent flow is about 10 to 60 times the diameter (Seif [18]).The velocity profile in the fully developed flow remains constant and is generally flatter compared to laminar flow where it is parabolic. Now it should be clear that, the flow through the pipe is different from that of a free stream. When an AUV moves inside a pipe, it experiences wall effects, especially in low diameter pipes. This causes an increase in resistance. The narrower the pipe diameter, the more the resistance. This added resistance should be calculated accurately, since it is necessary for the determination of vehicle speed, power demand, range and duration of operation. Another important parameter is the AUV diameter. According to the pipe diameter, the diameter of the AUV should be specified to obtain the minimum resistance.

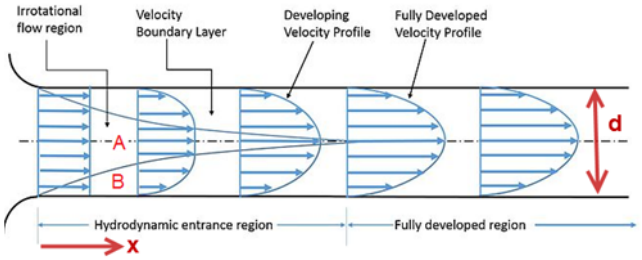

Figure 2. Boundary layer and velocity distribution inside a pipe in laminar flow

2. Specifications of the Model and pipe

The base model that is considered here is an axis-symmetric AUV similar to that of a torpedo, having no appendages since in the research is to study only the bare hull. This helps to halve CFD modeling of the body which would save time. The total length of the model is 2m, the diameter 0.25m, the wetted surface area 1.35m^2, the volume 0.08m^3 and the fineness ratio (L/D) is 8.The specifications of the model are presented in Figure 3.

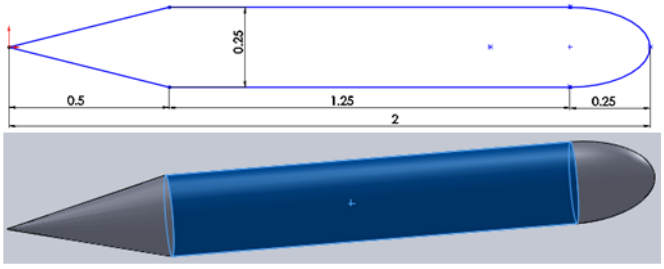

Figure 3. General configuration of the models

Inside dimensions of the model are constant, but the diameter of the tube (d) changes. For this study, according to Figure 4 and Table 1,ten different pipe diameters are considered (d/D=1.22, 1.41, 1.58, 1.73, 2, 3, 4, 10, 12 and 13). The ratio of the water section area (A_2) to the section area of the model (A_1) is crucial. Some of the d/D values are considered according to A_2/A_1. The values of d/D= 1.22, 1.41, 1.58 and 1.73 are respectively equivalent to A_2/A_1=0.5, 1, 1.5 and 2 respectively. Three different speeds are considered; 1, 3 and 10m/s. These speeds are considered so that all Reynolds number(ud/ν) valuesbe exceed 2300. This provides fully turbulent flow inside the pipe. The usual speed of AUVs inside the tube is in the range of 1~3m/s but the speed of 10m/s is considered for high speed vehicles such as the ejection of torpedo from the torpedo tube.

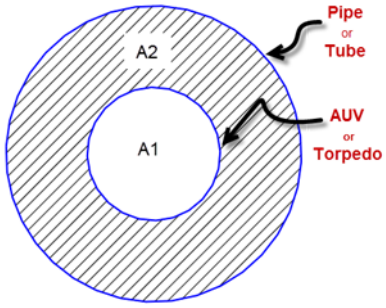

$A_1=\pi D^2/4$, $A_2=\pi/4(d^2-D^2)$

Figure 4. Cross section area of AUV and pipe (hatched area: water between AUV and pipe)

Table 1. Description of considered conditions

d (m)	d/D	A_2/A_1
0.304	1.22	0.5
0.36	1.41	1
0.394	1.58	1.5
0.432	1.73	2
0.5	2	2.9
0.75	3	7.8
1	4	14.7
2.5	10	97.1
3	12	140.3
3.25	13	164.8

3. CFD Method of Study

This analysis is performed by Flow Vision (V.2.3) software based on CFD method and solving the RANS equations. Based on the traditional Finite Volume concept and modern C^{++} implementation, Flow Vision is still very different from the competition. The Flow Vision workflow is more flexible and focused on solving physical problems rather than mesh generation. Meshing in Flow Vision is completely automatic and forms an integral part of a solver, which results in many benefits and unique capabilities. The Flow Vision development started in the late 90's at Russian Academy of Science and is continued since 1999 in the Capvidia group. Today Flow Vision evolved to the third generation product addressing wide range of applications often unique and not supported by traditional CFD products. Co-simulation with SIMULIA Abaqus has been pioneered for over 12 years resulting in powerful solution for heavily coupled FSI (Fluid Structure Interaction) problems as e.g. simulation of tires hydroplaning. High-level scalability of FlowVision parallel solver minimizes computational time scaling complex R&D simulations to practical engineering tasks. The multi-parameter optimization automates design processes to deliver optimal solutions which are impossible to get through traditional engineering practices (FVweb[19]).

3.1. Governing Equations

Transfer of momentum between layers is due to:

1) Viscosity or friction between fluid layers result in transfer of momentum from one fluid layer to another; this is a molecular level effect (due to rubbing of adjacent molecules).
2) Turbulent mixing resulting in additional apparent stress or Reynolds stresses (after Osburn Reynolds in 1880); this is a macroscopic effect due to bulk motion of fluid elements.

Momentum (Navier-Stokes) equation by using Einstein notation (sum each repeated index over i,j, and k) for Cartesian coordinates and the x-component where (x_i , x_j , x_k) = (x , y , z) and (u_i , u_j , u_k)= (u , v , w) are as eq. (1):

$$\rho\left[\frac{\partial(u_i)}{\partial t}+\frac{\partial(u_j u_i)}{\partial x_j}\right]=-\frac{\partial p}{\partial x_i}+\frac{\partial}{\partial x_j}\left(\mu\frac{\partial u_i}{\partial x_j}\right) \quad (1)$$

In terms of shear stress by using:

$$\tau_{ij}=\mu\left(\partial u_i/\partial x_j+\partial u_j/\partial x_i\right), \text{ or mean strain rate },$$

$S_{ij}=\tau_{ij}/(2\mu)$, the equation is reformed to Eq.(2):

$$\rho\left[\frac{\partial(u_i)}{\partial t}+\frac{\partial(u_j u_i)}{\partial x_j}\right]=-\frac{\partial p}{\partial x_i}+\frac{\partial \tau_{ji}}{\partial x_j} \text{ or} \quad (2)$$

$$\rho\left[\frac{\partial(u_i)}{\partial t}+\frac{\partial(u_j u_i)}{\partial x_j}\right]=-\frac{\partial p}{\partial x_i}+\frac{\partial}{\partial x_j}(2\mu S_{ji})$$

Mean and fluctuating velocities and pressure can be represented as:

$u_i(x,y,z,t) = \bar{u}_i(x,y,z) + u'_i(x,y,z,t)$ and $p(x,y,z,t) = \bar{p}(x,y,z) + p'(x,y,z,t)$.

Mean velocity is defined as:

$$\bar{u} = \frac{1}{T}\int_0^T u_t dt$$

Substitute in mean and fluctuating variables and expand to get the form of eq. (3):

$$\rho\left\{\frac{\partial(\bar{u}_i + u'_i)}{\partial t} + \frac{\partial\left[(\bar{u}_j + u'_j).(\bar{u}_i + u'_i)\right]}{\partial x_j}\right\} = -\frac{\partial(\bar{p} + p')}{\partial x_i} + \frac{\partial}{\partial x_j}\left[\mu\frac{\partial(\bar{u}_i + u'_i)}{\partial x_j}\right] \quad (3)$$

$$\rho\left[\frac{\partial\bar{u}_i}{\partial t} + \frac{\partial(u'_i)}{\partial t} + \frac{\partial(\bar{u}_j\bar{u}_i)}{\partial x_j} + \frac{\partial(\bar{u}_j u'_i)}{\partial x_j} + \frac{\partial(\bar{u}_i u'_j)}{\partial x_j} + \frac{\partial(u'_j u'_i)}{\partial x_j}\right] = -\frac{\partial\bar{p}}{\partial x_i} - \frac{\partial p'}{\partial x_i} + \frac{\partial}{\partial x_j}\left[\mu\frac{\partial\bar{u}_i}{\partial x_j} + \frac{\partial u'_i}{\partial x_j}\right]$$

Following rules would be applied on the equations:

$$\overline{\bar{u}_1} = \bar{u}_i\overline{\bar{u}_1 + u'_1} = \bar{u}_i + \overline{u'_i} = \bar{u}_i\overline{\bar{u}_1.u'_1} = \bar{u}_i.\overline{u'_j} = 0$$

$$\overline{\frac{\partial u_i}{\partial x_j}} = \frac{\partial\bar{u}_i}{\partial x_j}\overline{\bar{u}_i^2} = \bar{u}_i^2\overline{u'_i u'_j} < 0$$

$$\frac{\partial u}{\partial t} = \frac{\partial\bar{u}}{\partial t} + \frac{\partial u'}{\partial t}$$

$$\frac{\partial}{\partial x}(u^2) = \frac{\partial}{\partial x}[(\bar{u} + u')^2] = \frac{\partial}{\partial x}(\bar{u}^2 + 2\bar{u}u' + u'^2)$$

Many terms cancel to give Reynolds Averaged Navier Stokes (RANS) equations as eq. (4):

$$\rho\left[\frac{\partial\bar{u}_i}{\partial t} + \frac{\partial(\bar{u}_j\bar{u}_i)}{\partial x_j}\right] = -\frac{\partial\bar{p}}{\partial x_i} + \frac{\partial}{\partial x_j}\left[\mu\left(\frac{\partial\bar{u}_i}{\partial x_j}\right) - \rho\overline{u'_j u'_1}\right] \quad (4)$$

$$\rho\left[\frac{\partial\bar{u}_i}{\partial t} + \frac{\partial(\bar{u}_j\bar{u}_i)}{\partial x_j}\right] = -\frac{\partial\bar{p}}{\partial x_i} + \frac{\partial}{\partial x_j}\left(2\,\mu\bar{S}_{ji} - \rho\overline{u'_j u'_1}\right)$$

The term $(-\rho\overline{u'_1 u'_j})$ is named Reynolds stresses.

3.2. Condition "A"

This analysis is performed by Flow Vision (V.2.3) software based on CFD method and solving the RANS equations. Generally, the validity of the software results has been confirmed by several experimental test cases. The software, nowadays, is accepted as a practicable and reliable software in CFD activities. For the purpose of modeling these cases, Finite Volume Method (FVM) is employed. A structured mesh with cubic (hexahedral) cells has been used to map the space around the AUV. Transition of laminar layer to the turbulent layer in boundary layer, and flow separation are very important factors in resistance calculations. Y^+ and mesh numbers which to be selected with great care, are two significant parameters for modeling the boundary layer in CFD. For modeling the boundary layer near the solid surfaces, the selected cell near the object is very small compared to the other parts of the domain. In order to pick up the proper quantity of the cells, for one certain condition (d/D=1.41, A_2/A_1=1) and v=3m/s; seven different amount of meshes were selected and the results of resistance force of each were compared. The results remained almost constant after 1.9 millions of meshes, showing that the results are independent of the meshing (Fig.5). In all modeling the mesh numbers are considered more than 2.1millions.

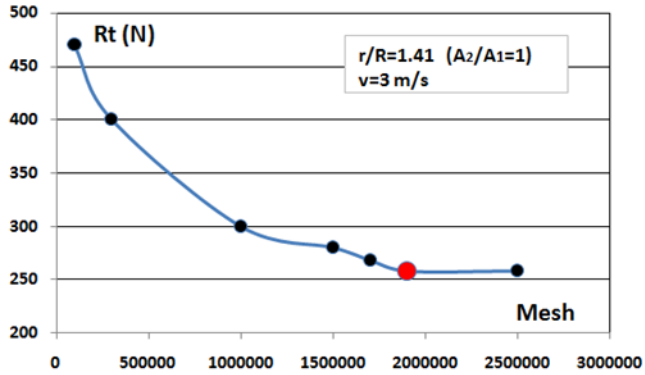

Figure 5. Mesh independency evaluations

Because of axis-symmetric shape and axis-symmetry of the flow current only a quarter of the body and the domain are modeled (Figure 6). In this domain, there is an inlet (with uniform flow), a free outlet, a symmetry (in the two faces of the symmetric plane) and a wall (for the body of AUV and for the pipe interior boundary). Domain length is equal to 7L (2L+L+4L) with several different diameters. The study assumes that the water inside the pipe is calm and having no speed and only the AUV moves. The turbulence model is K-Epsilon, turbulent scale is considered 0.1m and Y^+ is considered 30~100. The fluid is considered incompressible (fresh water) at 20 degrees centigrade and velocity of 1, 3, 10m/s. Settings of the simulation are collected in Table 2. Selection of the proper "time step" in each iteration, depends upon three parameters: speed, model length and mesh numbers along the main direction of movement, since the transfer of network is to be stopped on each section. For example, if v=1m/s, then the boundary layer will pass 2m length of the body in 2 seconds. The direction of velocity is along the axis, and for every 1 cm, one station of mesh is considered, that is 200 longitudinal station along the body (not all of the domain). For stopping the steam (flow) in each station, the time step is 2/200=0.01 seconds. On the other hand, the minimum time step required is

$$\left(\frac{\text{body length/speed}}{\text{longitudinal station numbers on the body}}\right).$$

Table 2. Settings of the simulation (inside the pipe)

Elements	Boundary conditions	Descriptions	
Domain	Cylinder (quarterly)	conditions	Fully submerged modeling (without free surface)- quarter modeling- domain with inlet, outlet, symmetry and wall- Without heat transfer.
		dimensions	A) length: 7L=2L+L+4L(distance before:2L- distance after: 4L) B) length: 6L=2L+L+3L (distance before:2L- distance after: 3L)*16R*16R C) length:10d+L+3L : distance before:10d- distance after: 3L
		grid	structured grid- hexahedral cells- without skew- fine cell near wall- Mesh numbers: A) more than 2.1 million B) 2 million C)2.8 million aspect ratio less than 3, expansion factor less than 1.7.
		settings	Cartesian coordinate system, Simulation time: 7 sec- Iterations more that 700- Time step=0.01sec.
Fluid	-	Incompressible fluid (water)- Reynolds number, is different in each pipe- turbulent modeling: Standard k-ε- fresh water- tempreture:20 deg- ρ=999.841 kg/m^3.	
Object	Wall	Bare hull of AUV- value 30<y$^+$<100 - logarithm wall function, roughness=0- no slip	
Input	Inlet	Velocity=1,3,10m/s- normal (along x)- in 1 face	
Output	Free outlet	Zero pressure- in 1 face	
Symmetry	Symmetry	In 2 faces	
Boundaries	Wall	For modeling the pipe wall- no slip condition	

In order to select the suitable iteration amount, the boundary layer should be considered in such a way that it could travel the whole domain, from the beginning to the end. As an example, if the full length of the domain be 21m, and v=3m/s, it needs 7 seconds to traverse the total length, and if "Time step=0.01sec" is considered, a minimum number of 7÷0.01=700 iterations is needed. These conditions are collected in Table 2.

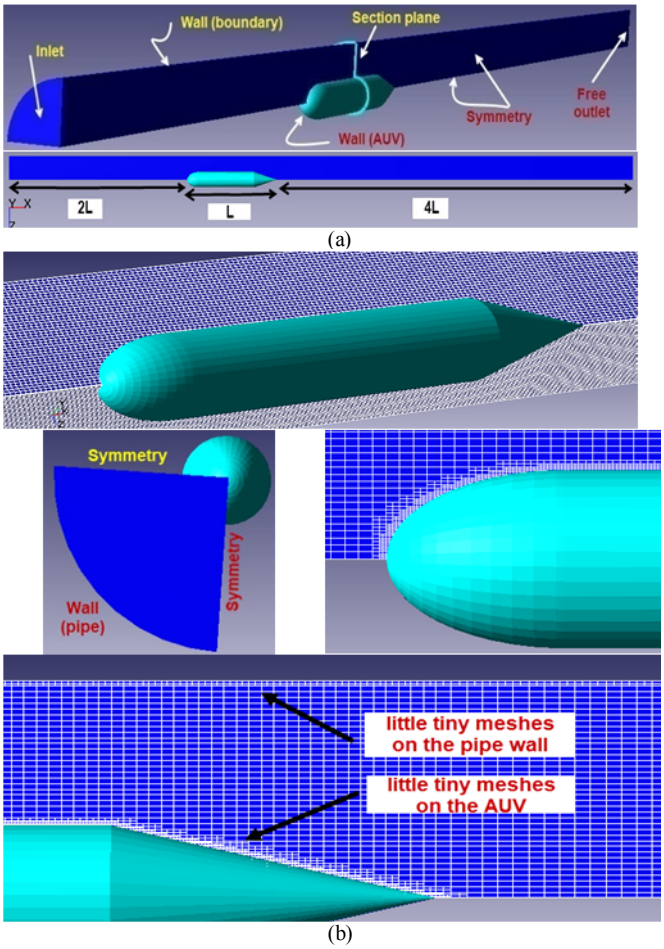

Figure 6.Condition A: (a) Domain and general dimensions (b) structured grid and Very fine cells near the wall for boundary layer modeling

3.3. Condition "B"

To analyze the pipe wall effect upon the resistance, it is needed to simulate the free stream, that is, no pipe and no wall effect. The domain and the simulation are shown in Figure 7. In this domain, there is an inlet (with uniform flow), a free outlet, a symmetry (in the four faces of the box) and a wall (for the submarine body). The domain is a box with dimensions of 12*2*2 m (or 6L*16R*16R). Mesh number is two millions.

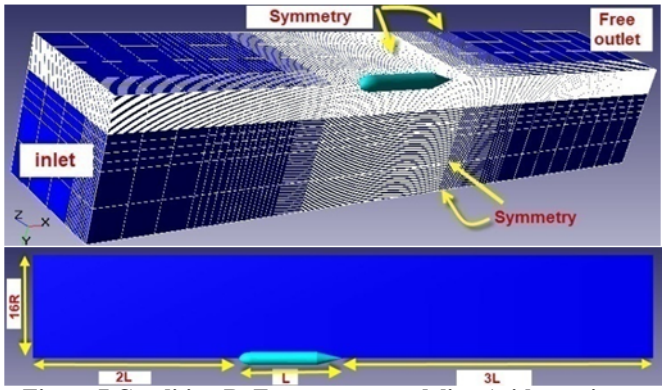

Figure 7.Condition B: Free stream modeling (without pipe wall effects)

3.4. Condition "C"

As mentioned above, the main assumption is that the water inside the pipe is calm and only the AUV moves, but if we regard that there is an initial water speed inside the pipe, the entrance length should be taken into account. To determine the forward distance, more "hydrodynamic entrance length" from the beginning of the pipe is required. As discussed before, the entry length in turbulent flow is about 10 to 60 times the diameter, and the turbulent flow occurs after Reynolds number(ud/ν) exceeds 2300. More turbulent flow induces lesser entrance length. At this point, this condition is studied only in one case: d/D=4 and v=1,3,10m/s. It is supposed that the AUV is constant and only the water moves. The flow is turbulent, and

the entrance length (forward distance) is minimally considered to be equaling "10d". Thus, the length of the cylindrical domain is "10d+L+3L"(Figure 8). This domain has a diameter of 1m and a length of 18m (10+2+6). Here, the mesh number is more than 2.8 million and there are little meshes far from the object. Other simulation conditions are similar to the ones mentioned before.

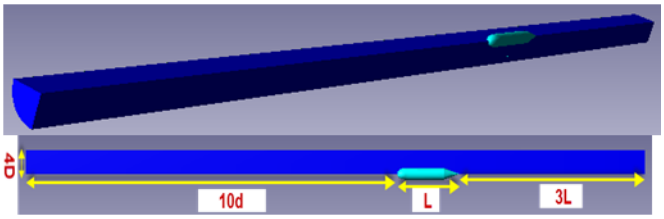

Figure 8.Condition C: Entrance length condition for d/D=4

4. CFD Results and Analysis

In this regard, two main factors should be discussed: 1)The pipe wall effects and 2)The fluid speed changes effects. Wall effect of the pipe causes some boundary layer effects on the fluid, and a zero speed just on the wall. Fluid speed change appears because of the limited cross section area between the body and the pipe. The minor distance between the body and the pipe, means minor cross section area (A_2). The fluid flux is constant, so the fluid speed should be increased. Increase in speed, according to Bernoulli's law, is equivalent to a decrease in pressure. For little values of A_2, the change in the fluid speed owing to the flux is more than the effect of the boundary layer on the pipe wall. Figure 9, shows the variation of pressure, for several values of d/D, in the cross section of the pipe. As the figure clearly shows an increase in A_2, induces an increase in average pressure of the fluid. Indeed, this comes as a result of a decrease in speed. In Fig.9a, the average pressure is -6530 (P_a) and in Fig.9d, it is 127 (p_a). In Fig.9a& 9b the form of pressure distribution is different from those of (c) and (d), because, as mentioned above, an increase in the pipe diameter brings about a decrease in the constant flux effect. In the next stage, the variation of resistance of the model (AUV) is discussed. The resistance for conditions A, B and C are represented. The total resistance (R_t) is the summation of the pressure resistance (R_p) and the viscous resistance (R_f). Here, the main factor causing a change in the resistance is the pressure resistance, because of it is wholly depended upon the pressure distribution over the body. In each stage, the total resistance and the pressure resistance are presented.

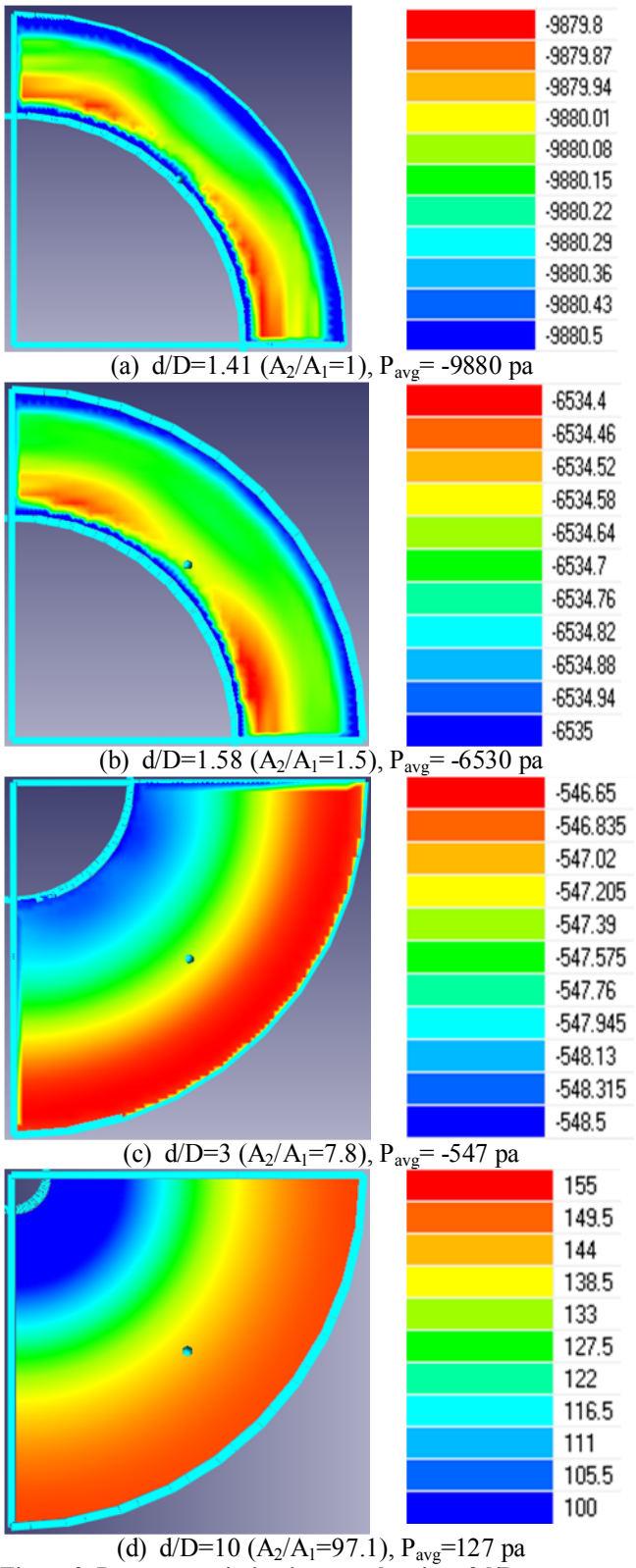

(a) d/D=1.41 (A_2/A_1=1), P_{avg}= -9880 pa

(b) d/D=1.58 (A_2/A_1=1.5), P_{avg}= -6530 pa

(c) d/D=3 (A_2/A_1=7.8), P_{avg}= -547 pa

(d) d/D=10 (A_2/A_1=97.1), P_{avg}=127 pa

Figure 9. Pressure variation in several ratios of d/D

4.1.Condition "A" and "B"

The total resistance and the pressure resistance of AUV in several different diameters of tubes are presented in the Table 3 and Figure 10. These results are presented for three speeds of 1, 3 and 10m/s. Clearly at all speeds where d/D<1.41 (or A_2/A_1<1), there is a jump in the resistance diagram. Therefore, it can be suggested that in all pipes or torpedo tubes, the following should be considered d/D>1.41 (or A_2/A_1>1). In swim out (self-

propelled) system of torpedoes, in submarines, the torpedo diameter is 533mm and torpedo tube (launcher) is 640mm, which eventuate A_1=0.223m^2 and A_2=0.0985m^2. For easier ejection of torpedo from the tube, a minimum tube diameter of 750mm, can be recommended which provides A_1=A_2. The main limitation for increasing the tube diameter is the architecture arrangement inside a submarine or naval ship, and the required volume of water to fill the space dimension between torpedo and the tube. This volume of water must be kept up in the submarine tanks, but in pipelines, there is no such restriction. The diameter of AUV can be designed according to the diameter of the pipe. The diagrams of Figure 10 shows that, when d/D=1.41, there is a mild variation in resistance. Logically, by increasing the pipe diameter, the decrease in resistance values is observed.

Table 3. Values of total resistance and pressure resistance

d/D	v=1m/s		v=3 m/s		v=10 m/s	
	Rt (N)	Rp (N)	Rt (N)	Rp (N)	Rt (N)	Rp (N)
1.22	145.2	125.2	1110.8	963.6	12820	11624
1.41	34.8	26.4	258	198	2392	1838
1.58	22	15.6	160.8	114	1099.2	820
1.73	15.2	10	115.2	76	1075.2	715.6
2	10.4	6	78.4	46.4	741.2	445.6
3	7.2	4	50.4	26	490	266
4	6	3	46	23.6	444	238
10	6	3.36	37.6	16.8	358	172
12	4.6	2	36.8	17.2	352.4	166
13	4.6	2	36.6	16.8	348	158
infinitive	4.6	2	36.6	16.8	348	158

At the speeds of 1m/s and 3m/s, the results after d/D=12 remain constant. The values of "d/D=infinitive" is related to condition "B" which models the free stream condition. That is, after this limit, the added resistance and the pipe wall effect is negligible. This diameter is the "Critical diameter". At the speed of 10m/s, the critical diameter happens in d/D=13. However, since there is no high speeds in pipes, one can conclude that d/D=12 is related to the critical diameter. The ratio of pressure resistance to the total resistance is shown in Figure 11. As mentioned above, the pressure resistance has a unique role in the total resistance. This diagram shows that when the value of d/D<1.41, the pressure resistance is about 90 percent of the total resistance. In the infinitive diameter (d/D=infin.), this value is about 45 percent. That is to say, the wall effect of the pipe has induced the pressure resistance to be twice as much. By increasing the diameter, the percentage of the pressure resistance decreases gradually.

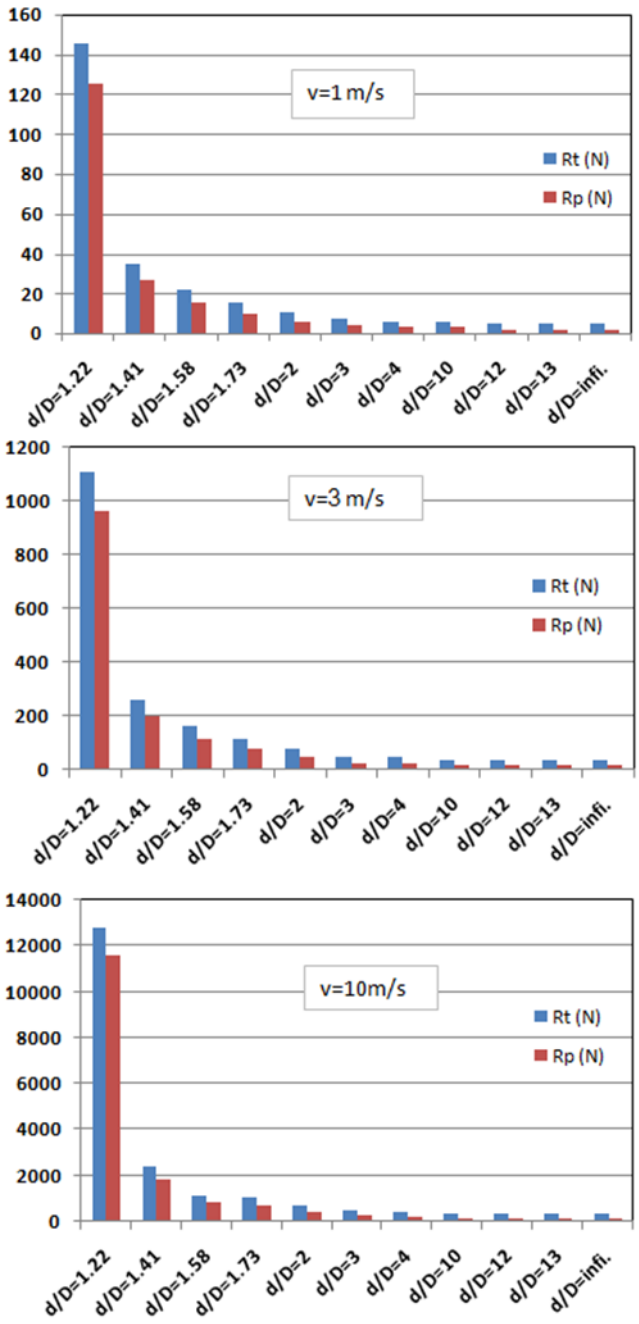

Figure 10. Total resistance and pressure resistance of AUV in several different d/D and speed

To interpolate other values of d/D, the best curve is fitted to these points by Curve expert software (Figure 11). The extracted formula is as eq.5:

$$\frac{R_p}{R_T} = \frac{43.5\,(d/D)}{-0.61 + (d/D)} \qquad (5)$$

For a better understanding ofthe pipe wall effect on resistance, the ratio of total resistance to free stream resistance (condition C) is represented in Figure 12. The amount of R_t/R_0=1, shows that when the wall effect is deleted, free stream condition obtains.

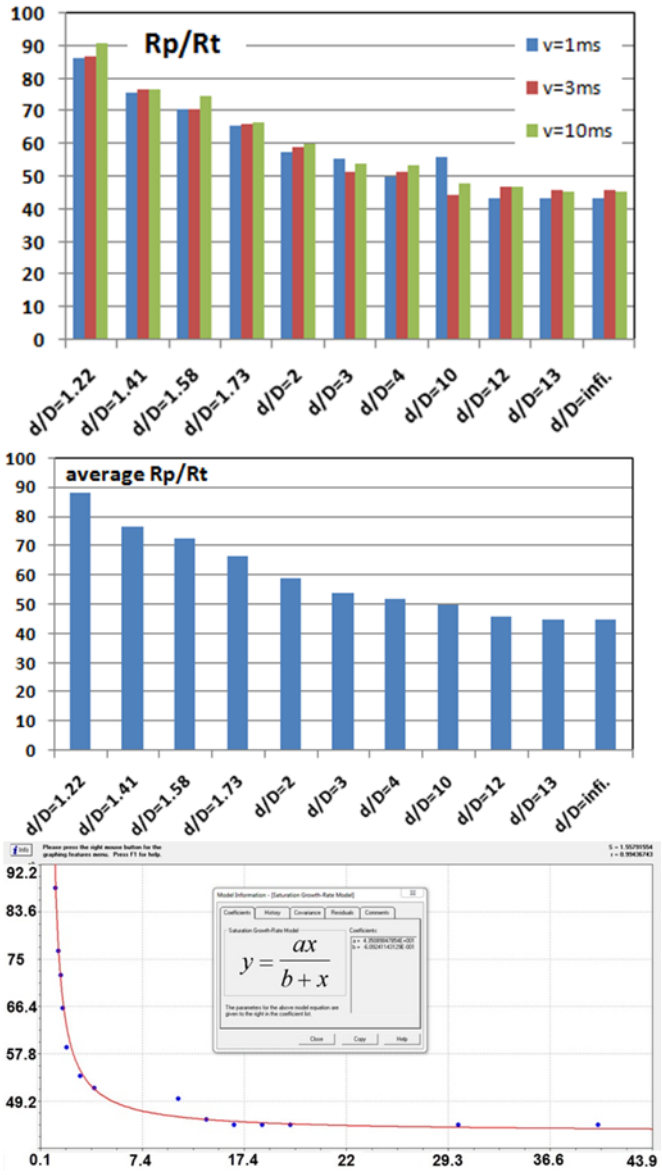

Figure 11. The ratio of pressure resistance to total resistance

To interpolate other values of d/D, the best fitted curve is shown in Figure 12, and the related formula is as Eq.6:

$$\frac{R_T}{R_0}=\frac{1.01}{1-2.06e^{-0.62(d/D)}} \qquad (6)$$

As mentioned before, the ratio of d/D=12 can be regarded for critical diameter, neglecting the added resistance and the pipe wall effect.

4.2. Condition "C"

The comparison between the results of condition A and C is presented in Table 4. The results show a decrease of about 5 percent in the total resistance, and 10~20 percent decrease in the pressure resistance. The reason for the decrease is a reduction in the fluid speed, coming about as a result of flow development and the boundary layer expansion after the entrance length. That is, if it is assumed that the fluid is not calm and it has an initial speed, then the entrance length should be regarded for developing the boundary layer taking into account an approximate five-percent decrease in the total resistance. In condition A, there is no entrance length, and the boundary layer is not developed. As a rule, in engineering problems, in order to inspect the pipelines, no initial flow speed is considered, for by conducting the inspections and repairs, the valves are closed.

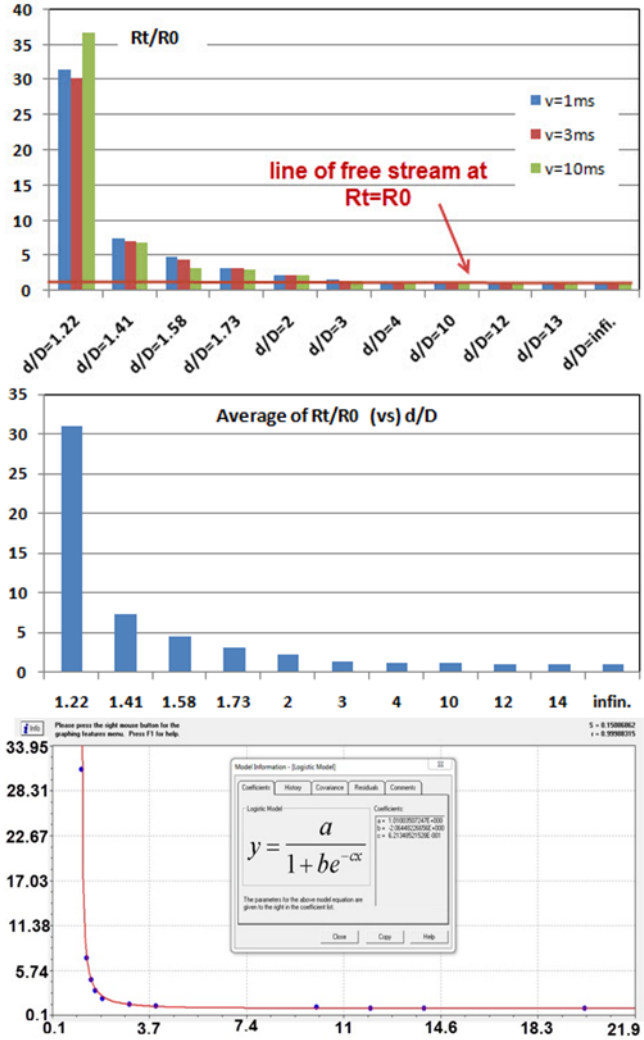

Figure 12. Ratio of total resistance to free stream resistance

Table 4. Comparison of results for d/D=4

	V=1m/s		v=3m/s		v=10m/s	
	Rt	Rp	Rt	Rp	Rt	Rp
Condition "A"	1.5	0.75	11.5	5.9	111	59.5
Condition "C"	1.4	0.6	10.9	5.1	107	53.3
Decrease percentage (%)	6.67	20	5.22	13.56	3.60	10.42

5- Conclusion

To conclude, as regards the added resistance due to wall effect, for an AUV moving inside a pipe,the following can be mentioned: Pressure resistance play a major role in the total resistance. The ratio of d/D=12 can be regarded for the determination of the "critical pipe diameter" in which the added resistance is zero.The ratio of d/D<1.41 (or $A_2/A_1<1$) causes a stiff increase along with the resistance. Therefore, the values below this ratio is not recommended.In swim out system of torpedo launching, in the case of

533mm torpedoes, the minimum tube diameter of 750mm is recommended. If there is an initial water speed inside the tube, the entrance length and the developed boundary layer should be regarded.

Nomenclature

A_1	Section area of the model
A_2	Section area of water between model and pipe wall
AUV	Autonomous Underwater Vehicles
Cf	Frictional resistance coefficient
Cp	Pressure resistance coefficient
Ct	Total resistance coefficient
CFD	Computational Fluid Dynamics
D	Maximum diameter of AUV (m)
d	Diameter of pipe (m)
IHSS	Iranian Hydrodynamic Series of Submarines
L	Overall length of hull (m)
l	Overall length of pipe (m)
P_{avg}	Average Pressure of fluid between pipe and model (pa) (all pressures are relative = $P-P_{atm}$)
Re	Reynolds number
Rf	Frictional resistance (N)
Rp	Pressure resistance (N)
Rt	Total resistance (N)
R_0	Total resistance in free stream (without pipe wall stream) (N)

References

1- Painumgal,U.V.; Thornton,B.; Uray, T.; Nose,Y.; (2013), *Positioning and Control of an AUV inside a water pipeline for non-contact in-service Inspection*, IEEE, 978-0-933957-40-4, p.542-552.

2- Majjid. M. Moghaddam, AlirezaHadi, (2005), *Control and Guidance of a Pipe Inspection Crawler (PIC),* 22nd International Sysnposium on Automation and Robotic s in Construction.

3- Harry T. Roman, Bruce A. Pellegrino, (1993), *Pipe Line Crawling Inspections:An Overview, IEEE Transactions on Energy Conversion*, Vol. 8, No.3, p.2196-2203.

4- Bahmanyar S, Yousefi-Koma A, Ghasemi H. (2011), *Development of a robot fish with experimental analysis*, 3; 7 (13) :49-65
URL http://www.ijmt.ir/browse.php?a_code=A-10-13-1&slc_lang=en&sid=1

5- M.Muramatsu, N. Namiki, R. Koyama, Y. Suga, (2000), *Autonomus Mobile Robot in Pipe for Piping Operations*, IEEE International Conference on Intelligent Robots and Systems, pp. 2166-2171.

6- Roh, S.G.; Ryew, S.M.; Yang, J.H.; Choi, H.R., (2001), *Actively steerable in-pipe inspection robots for underground urban gas pipelines*, IEEE International Conference on Robotics and Automation, vol.1, pp. 761 - 766.

7- Roh, S.G.; HyoukRyeol Choi, (2005), *Differential-drive in-pipe robot for moving inside urban gas pipelines*, IEEE Transactions on Robotics and Automation, Volume 21,Issue 1, pp. 1 - 17.

8- DadkhahKhiabani E, M. Gharabaghi A R, Abedi K. (2013), *Investigation into the Effects of Buckle Arrestors on the Arresting of Dynamic Buckle Propagation in Pipelines*. 3; 8 (16) :19-31
URL http://www.ijmt.ir/browse.php?a_code=A-10-164-1&slc_lang=en&sid=1

9- Okamoto. Jun, Julio C. Adamowskia, Marcos S.G. Tsuzukia, FlavioBuiochia, Claudio S. Camerinib, (1999), *Autonomous system for oil pipelines inspection*, Mechatronics , Elsevier, pp. 731-743(13).

10-P.N.Joubert, (2004), *Some aspects of submarine design: part 1: Hydrodynamics*, Australian Department of Defence.

11- P.N.Joubert, (2004), "*Some aspects of submarine design: part 2: Shape of a Submarine 2026*", Australian Department of Defence.

12- Moonesun M, Korol Y, Dalayeli H., (2015), *CFD Analysis on the Bare Hull Form of Submarines for Minimizing the Resistance*. 2 (3) :1-16
URL http://www.ijmt.ir/browse.php?a_code=A-10-450-1&slc_lang=en&sid=1

13- Moonesun.M, (2014), *Introduction of Iranian Hydrodynamic Series of Submarines (IHSS),* Journal of Taiwan society of naval architecture and marine engineering , Vol.33, No.3, pp.155-162.

14- R.Burcher, L.J.Rydill, (1998), *"Concept in submarine design*", The press syndicate of the University of Cambridge., Cambridge university press, pp. 295.

15- H.Najjaran, (2005), *IRC creating an underwater robotic vehicle to inspect inservice water mains*, Construction Innovation, vol. 10, no. 2.

16- JorgKalwa, (2012), *SeaCat AUV Inspects Water Supply Tunnel, Sea Technology Magazine* http://www.seatechnology.
com/features/2012/0812/seaCat.php.

17- http://pritamashutosh.wordpress.com/2014/02/06/flow-through-circular-conduits/

18- M.S.Seif, (2012), *Fluid Mechanics*", Fadak publication, Iran.

19- *Flow Vision website*: https://fv-tech.com/index.php/en/